

# CONTROL OF ROTOR-BLADE COUPLED VIBRATIONS USING SHAFT-BASED ACTUATION

**René Hardam Christensen**

Department of Mechanical Engineering, Technical University of Denmark, DK-2800 Kgs. Lyngby, Denmark  
rhc@mek.dtu.dk

**Ilmar Ferreira Santos**

Department of Mechanical Engineering, Technical University of Denmark, DK-2800 Kgs. Lyngby, Denmark  
ifs@mek.dtu.dk

**Abstract.** *When implementing active control into bladed rotating machines aiming at reducing blade vibrations, it can be shown that blade as well as rotor vibrations can be controlled by the use of only shaft-based actuation, if the blades are deliberately mistuned. This paper investigates the dynamical characteristics of a mistuned bladed rotor and shows how, why and when the bladed rotor becomes controllable and observable due to the deliberate blade mistuning. The modal controllability and observability of a tuned as well as a mistuned coupled rotor-blade system are analysed. The dependency of the degrees of controllability and observability on varying rotational speed and mode shape interactions between parametric and basis mode shape components are also analysed. Numerical results reveal a limitation of the achievable controllability and observability, once quantitative measures of modal controllability and observability converges toward steady levels as the degree of mistuning is increased. Finally, experimental control results are included to prove the theoretical conclusions and to show the feasibility of controlling rotor and blade vibrations by means of shaft-based actuation in practice.*

**Keywords.** *controllability, periodic system, bladed disc, periodic modal analysis.*

## 1. Introduction

The implementation of active vibration control into bladed rotating machines such as for instance turbo machinery implies that sensors and actuators will have to be built-in monitoring the vibration levels and applying proper control action based on the measurements. Sensors can, though not easily, be built into the rotating blades to monitor their vibration levels, i.e. by using strain gages (Al-Bedoor, 2002). Alternative methods to measure the blade vibration levels by using sensors fixed in the non-rotating frame have also been developed to avoid sensors built into the blades, requiring signal transmission from a rotating to a non-rotating frame by using slip-rings or telemetric devices and also requiring high resistance to tough working conditions (Zielinski, 2000). Building actuators into rotating blades is more complicated than implementing sensors. The only feasible actuation technique to be built into each individual blade is the use of smart materials, i.e. piezo-electric elements, which can also be used as sensing elements. However, it will be very costly and introduce many difficulties to be overcome, if a piezo-electric actuation/sensing element should be embedded into each individual blade. Active controlled bearings for rotor vibration control have been developed for many years and applied for various purposes, for example active magnetic bearings (Schweitzer, 1998), active lubricated bearings (Santos and Scalabrin, 2003), piezo-actuated bearings (Alizadeh et al., 2003) or bearings controlled by means of hydraulic actuators (Althaus and Ulbrich, 1992). Therefore, one could ask: Are actuators built into the blades absolutely required in order to control rotor blade vibrations? Can the rotor as well as blade vibrations be monitored and controlled by means of shaft-based sensing and actuation solely?

Such questions have been studied by very few researchers. In the work of Szász and Flowers (2000) the controllability of a bladed disk was analysed by studying its vibration mode shapes. It was shown that a tuned bladed disk can not be controlled by using only shaft-based actuation and sensing. However, if properly mistuned it was shown that the disk becomes controllable. Numerical control results of a mistuned disk controlled via shaft-based actuation were described in that work and in (Szász et al., 2000; Szász and Flowers, 2001). The controllability analysis was based on studying only time-invariant mode shapes while the time-variant vibration modes, known as parametric modes, which will occur due to vibration coupling between rotor and blades, were not considered. Therefore, in those cited works the blade vibrations are controlled by forcing the rotor/disk motion to minimize the blade deflections. For some rotating bladed systems where blade flexible motion is coupled to rotor lateral motion it might be possible to influence blade vibration levels by shaft-based actuation. If blade motion is coupled to rotor motion then blade vibration energy can be absorbed via controlling the motion of the rotor. Therefore, for bladed rotors presenting significant vibration coupling between rotor and blades such coupling and the presence of parametric coupled modes are very important to consider when analysing the system controllability. A methodology for studying the modal controllability and observability of a bladed disk, considering the rotor and blade vibration coupling, was presented in (Christensen and Santos, 2004c) and a tuned bladed disk was numerically analysed. Active control of a mistuned bladed rotor via shaft-based actuation was studied theoretically as well as experimentally in (Christensen and Santos, 2004a,b).

In this paper the modal controllability and observability of a coupled bladed rotor are analysed. It is aimed to show

why and how the introduction of deliberate blade mistuning makes the bladed rotor controllable and observable using only shaft-based actuation and sensing. Due to the presence of parametric modes, which depend on the rotational speed, and the interaction between basis and such parametric vibration modes at certain speeds, the degrees of controllability and observability will be dependent on the speed as well. Consequently, the influence of the rotational speed on the degrees of controllability and observability are also studied. Finally, the feasibility of controlling blade vibrations in a significantly coupled rotor-blade system by means of shaft-based active control is examined experimentally.

## 2. Rotor-blade system description and test facilities

Figure 1(a) shows a schematic drawing of the considered actively controlled coupled rotor-blade system. Four flexible blades are radially attached onto a rigid disk/shaft supported by active controlled radial bearings. Tip masses are added to the blades to emphasize their inertia and the vibration coupling among rotor and blades. It is noticed that the movement of the rotor is assumed to be restricted into the  $xy$ -plane neglecting rotor angular movements and gyroscopic effects. Such assumption simplifies the mathematical model describing the dynamics of the system and for the theoretical analysis of this work, this will be a permissible assumption. However, small rotor angular movements can not be completely avoided in practical machines but the experimental test rig built for this study, shown in Fig. 1(b), is designed to minimize the influence of such effects. For practical use in real bladed rotating machinery rotor angular movements and gyroscopic effects may have to be considered.

The experimental test rig is composed of the four bladed rigid disk mounted in a flexible suspension to allow significant rotor lateral movement. The rotor is driven by an electro-motor transmitting its torque through a pulley and two flexible couplings. Inductive non-contact measurement probes are attached to the rig to monitor the rotor/shaft lateral motion. Strain gages are bonded onto each blade to measure their deflections. Analog signal conditioning electronic circuits are built into the rigid disk for amplifying and filtering the strain gage signals. The measured signals are transmitted from the rotating disk to a control unit through a slip-ring assembly. Two pairs of electro-magnetic actuators are applied to act onto the flexible suspension to control the rotor lateral motion, working like an active bearing. Sensors and actuators are connected to a digital signal processor dSPACE DS-1103 PPC controller board hosted on a PC, for data acquisition and for running control algorithms.

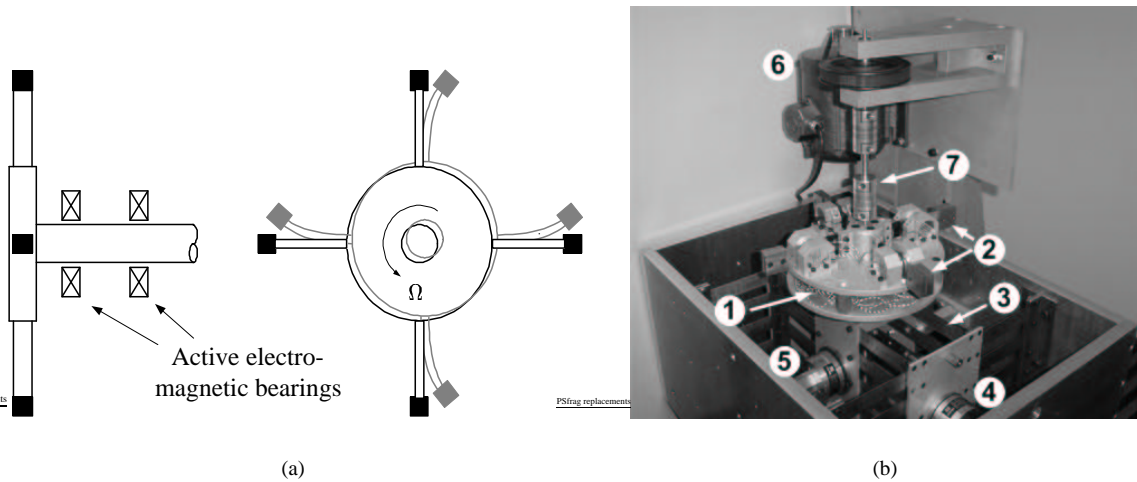


Figure 1: Schematic drawing (a) showing the active controlled rotor-blade system and a photograph (b) showing the experimental test facilities. **1** rotor disk; **2** rotor blades; **3** flexible suspension; **4** electro-magnetic actuator  $x$ -direction; **5** electro-magnetic actuator  $y$ -direction; **6** AC-motor; **7** pulley and flexible couplings.

## 3. Mathematical modelling

Due to the cyclic variation of the blade inertia distribution in time domain and the influence of centrifugal and coriolis effects, the general equations of motion for the coupled rotor-blade system are time-variant depending on rotor position, rotational speed and acceleration. For a details on the mathematical modelling and rotor-blade dynamical characteristics, see (Santos et al., 2004). Rotating at constant speed the model complexity reduces to become periodic time-variant with rotational speed  $\Omega$ . Using the state-space formulation the equations of motion are written as:

$$\dot{\mathbf{x}}(t) = \mathbf{A}(t)\mathbf{x}(t) + \mathbf{B}(t)\mathbf{u}(t) + \mathbf{F}(t) \quad (1)$$

$$\mathbf{y}(t) = \mathbf{C}\mathbf{x}(t) \quad (2)$$

where  $\mathbf{x}(t)$  is the vector of state variables,  $\mathbf{u}(t)$  is the vector of control forces acting onto the structure, applied via the active bearings.  $\mathbf{A}(t)$  denotes the periodic system matrix,  $\mathbf{B}(t)$  the control input matrix and  $\mathbf{F}(t)$  is a vector internal forces caused by the presence of the centrifugal and coriolis effects. The output matrix  $\mathbf{C}$  is defined so that the measured outputs  $\mathbf{y}(t)$  are the shaft lateral position.

By using a periodic modal coordinate transformation, the state-space model Eq. (1) and (2) is transformed into a modal form, more suitable for system analysis purpose and controller design. Due to the time-periodicity of the system, a classical time-invariant modal coordinate transformation can not be applied. Hence, a periodic modal transformation method will be used (Xu and Gasch, 1995). The efficiency of applying such modal transformation, not only for controller design purpose (Christensen and Santos, in press), but also for analysis of coupled rotor-blade systems and for mathematically to explain the presence of parametric vibrations of such systems were studied in (Saracho and Santos, 2003).

The modal model consists of a system of independent equations of motion, where each equation represents one vibration mode. It is derived by introducing a vector of modal state variables  $\xi(t)$ , defined by  $\mathbf{x}(t) = \mathbf{R}(t)\xi(t)$ , where  $\mathbf{R}(t)$  is the right modal matrix. Introducing this new vector of state variables, the system is rewritten into the form:

$$\dot{\xi}(t) = \mathcal{A}\xi(t) + \mathcal{B}(t)\mathbf{u}(t) + \mathcal{F}(t) \quad (3)$$

$$\mathbf{y}(t) = \mathcal{C}(t)\xi(t) \quad (4)$$

where  $\mathcal{A} = [\mathbf{L}^T(t)\mathbf{A}(t)\mathbf{R}(t) - \mathbf{L}^T(t)\dot{\mathbf{R}}(t)]$  is a constant matrix containing the basis eigenvalues of  $\mathbf{A}(t)$  along the diagonal,  $\mathcal{B}(t) = \mathbf{L}^T(t)\mathbf{B}(t)$  is the periodic oscillatory modal control matrix,  $\mathcal{F}(t) = \mathbf{L}^T(t)\mathbf{F}(t)$  is the periodic oscillatory vector of modal forces and  $\mathcal{C}(t) = \mathbf{C}\mathbf{R}(t)$  is the periodic modal output matrix.

The transformation matrices  $\mathbf{R}(t)$  and  $\mathbf{L}^T(t)$  denote the periodic complex right respectively left modal matrix of the system  $\mathbf{A}(t)$ . They are determined by solving a time-variant eigenvalue problem using Hill's method of infinite determinants. Introducing the solution  $\mathbf{x}(t) = \sum_{k=1}^{2N} \mathbf{r}_k(t)e^{\lambda_k t}$  into the equations of motion Eq. (1) yield an eigenproblem given by  $\dot{\mathbf{r}}_k(t) + [\lambda_k \mathbf{I} - \mathbf{A}(t)]\mathbf{r}_k(t) = \mathbf{0}$  where  $\lambda_k$  denotes the  $k$ 'th eigenvalue associated to the right hand eigenvector  $\mathbf{r}_k(t)$ . Expressing the periodic terms of the matrix  $\mathbf{A}(t)$  and the eigenvectors  $\mathbf{r}_k(t)$  by means of Fourier series, the periodic eigenvalue problem is transformed into a time-invariant form. By solving this problem the eigenvectors are determined in terms of its Fourier expansion coefficients, i.e.  $\mathbf{r}_k(t) = \sum_{j=-n}^n \mathbf{r}_{k,j} e^{ij\Omega t}$ . More details on how to set this up and how to solve it, i.e. separating basis and redundant solutions, are carefully described in (Xu and Gasch, 1995). The right modal matrix is given by the form:

$$\mathbf{R}(t) = \mathbf{R}(t+T) = \sum_{j=-n}^n \mathbf{R}_j e^{ij\Omega t} \quad (5)$$

where the Fourier coefficients are composed of the eigenvector coefficients  $\mathbf{R}_j = [\mathbf{r}_{1,j}, \mathbf{r}_{2,j}, \dots, \mathbf{r}_{2N,j}]$ . The Fourier coefficients  $\mathbf{R}_j$  represent basis and parametric vibration mode shape components of the system. The basis mode shapes, corresponding to the eigenvalues  $\lambda_k$ , are given by  $\mathbf{R}_0$  and parametric vibration mode shapes of order  $j$  are given by  $\mathbf{R}_j$ , corresponding to the eigenvalues  $\lambda_k + ij\Omega$ .

It is worth to mention that because of the non-symmetric form of the matrix  $\mathbf{A}(t)$  the right and left eigenvectors  $\mathbf{r}_k(t)$  and  $\mathbf{l}_k(t)$  are distinct, otherwise if  $\mathbf{A}(t)$  had been symmetric  $\mathbf{r}_k(t)$  and  $\mathbf{l}_k(t)$  would be equal and  $\mathbf{R}(t) = \mathbf{L}(t)$ . The left modal matrix is determined so that the orthogonality relation is fulfilled  $\mathbf{R}(t)\mathbf{L}^T(t) = \mathbf{I}$ , that means it is written by the expansion  $\mathbf{L}(t) = \sum_{j=-n}^n \mathbf{L}_j e^{ij\Omega t}$ .

#### 4. Measures of modal controllability and observability

In order to check the ability of the active bearings and shaft position sensors to control and monitor the rotor and blade vibration levels, the controllability and observability are analysed. The modal controllability and observability can be analysed by checking the modal control input matrix  $\mathcal{B}(t)$  and the modal output matrix  $\mathcal{C}(t)$ . General speaking, the system is, to some degree, modal controllable if no row of the modal control input matrix consists only of zeros and all modes are, to some degree, observable if no column of the modal output matrix consists only of zeros. Based on these facts, quantitative measures describing the degrees of controllability and observability of a specific mode, from all control actions and measurements can be deduced. Such measures are the so called gross measures of modal controllability and observability defined for time-invariant systems by Hamdan and Nayfeh (1989). Due to the time-variability of the rotor-blade system, resulting in time-variant eigenvectors, such measures for the actual system are given by their minimum values throughout one period of rotation, that is:

$$\text{GMC}_k(t) = \min \left[ \text{norm} \left[ \frac{\mathbf{l}_k^T(t) \cdot \mathcal{B}(t)}{\|\mathbf{l}_k^T(t)\|} \right] \right] \quad (6)$$

$$\text{GMO}_k(t) = \min \left[ \text{norm} \left[ \frac{\mathcal{C} \cdot \mathbf{r}_k(t)}{\|\mathbf{r}_k(t)\|} \right] \right] \quad (7)$$

where  $\mathbf{r}_k(t)$  and  $\mathbf{l}_k^T(t)$  are the  $k$ 'th right and left eigenvector, respectively. Basically, these measures are obtained as the norms of the rows and columns of the modal input and output matrices normalized by the lengths of the eigenvectors. The measures are directly related to the angles between the eigenvectors and the rows/columns of the input and output matrices.

## 5. Numerical results

### 5.1. Tuned system analysis

Figure 2 presents waterfall diagrams showing system frequency responses as function of the rotational speed. Such responses are obtained by applying fast fourier transformation to numerical calculated time responses of the rotor and blade movement, respectively. The diagrams clearly show the peculiarities characterizing the dynamics of this special kind of system. The presence of parametric vibration modes, due to the vibration coupling among the rigid disk/shaft and the flexible blade motions (Santos et al., 2004), is observed by the v-shaped frequency components. Figure 3 shows the frequency components present in the waterfall diagrams and the relation of each component to its respective vibration mode. The number denote the number of the specific mode and the letter M denotes basis modes while P, R and V denote parametric mode components. For instance, the components R1 and R2 are backward rotating contributions of order 1 from the rotor natural frequencies to the blade movement while P1 and P2 are forward rotating contributions of order 1 to the blade movement. The components R5 and P6 are backward respectively forward rotating contributions of order 1 from the blade natural frequency to the rotor movement. The component V5 is a backward rotating parametric mode shape component of order -2. The centrifugal stiffening is observed by the increasing blade eigenfrequencies with rotational speed, see M3, M4, M5 and M6 in Fig. 3. The remaining frequency components M1 and M2 are the disk/shaft lateral movement natural frequencies in the  $x$  and  $y$  direction, respectively.

Due to the velocity dependency of the frequencies of the parametric mode components, these will at certain velocities interact with the basis mode components. The parametric mode shape components and the basis mode components tend to converge towards each other at the velocities  $\sim 200$  rpm and  $\sim 350$  rpm denoted as transition regions (A) and (B). At these specific angular velocities the natural frequencies of the system and the mode shapes will converge, interact and then veer apart without crossing. Such phenomenon, known as frequency veering (Kenyon et al., 2004), can be detected among the basis modes and the parametric mode components of order  $\pm 1$  and  $-2$ . Due to this frequency veering, the natural frequency of the basis mode component denoted by M5 will not, in fact, correspond to the fifth mode at all velocities. Dependent on the specific angular velocity it will, in fact, be the third, fifth or sixth mode. Though, throughout this study this particular mode will be denoted as the fifth mode, related to its mode number of the non-rotating system.

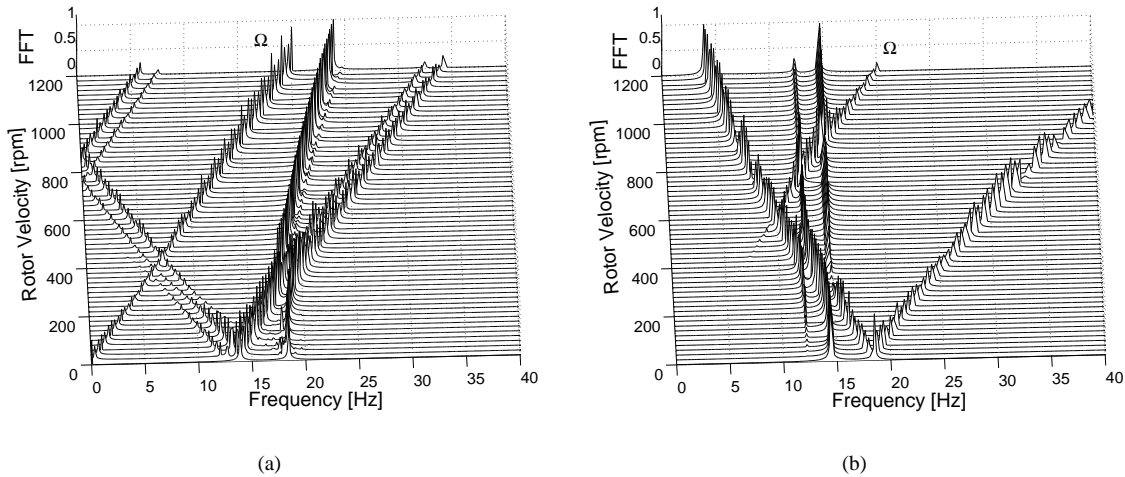


Figure 2: Waterfall diagrams of the blade (a) and rotor movement (b) for the tuned rotor-blade system.

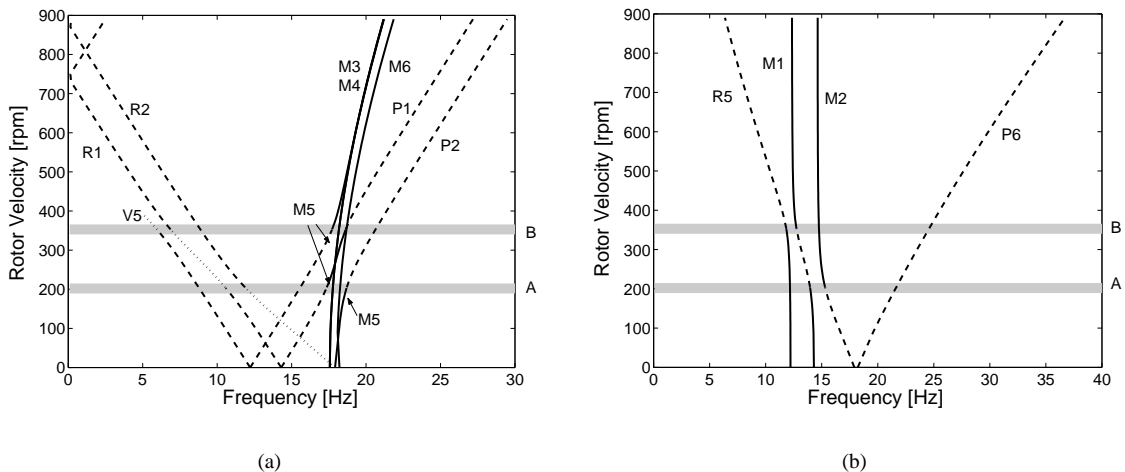


Figure 3: Basis (—) and parametric eigenvalues of order  $\pm 1$  (---) and of order  $-2$  ( $\cdots$ ) for the blade (a) respectively rotor movement (b).

As it was theoretically explained by the modal model and observed in the Figs. 2 and 3, the vibration mode shapes vary with rotational speed, due to the centrifugal stiffening and the parametric mode components. Consequently, the gross measures of modal controllability and observability, determined by using the time-variant eigenvectors, will vary as well. Figure 4 shows minimum values of the quantitative measures of modal controllability and observability through one period of rotation for the first six modes of the tuned rotor-blade system as functions of the rotational speed. The bladed disk is controlled and monitored by using only shaft-based actuation and sensing. The higher an index is, the more controllable or observable is the mode. If the index is zero then the mode is non-controllable or non-observable. The results show that if only shaft-based actuation and sensing are applied, only the modes 1, 2, 5 and 6 can be controlled and observed. The modes 3 and 4 can neither be controlled nor be observed by using shaft-based actuation and sensing, once the controllability and observability indices of such modes are zero.

Observing the the controllability and observability indices in Fig. 4 it is worth to notice the indices during the mode shape crossing regions (A) and (B). At these particular regions the indices of the crossing modes, 2 crosses 5 at (A) and 1 crosses 5 at (B), seems to converge towards similar values. More precisely, they converge as the velocity nears the transition velocity. The reason to this behaviour is, that the mode shapes when the velocities nears the transition phase tend to converge towards "identical" shapes. This can be observed by analysing the eigenvectors during the transition phase.

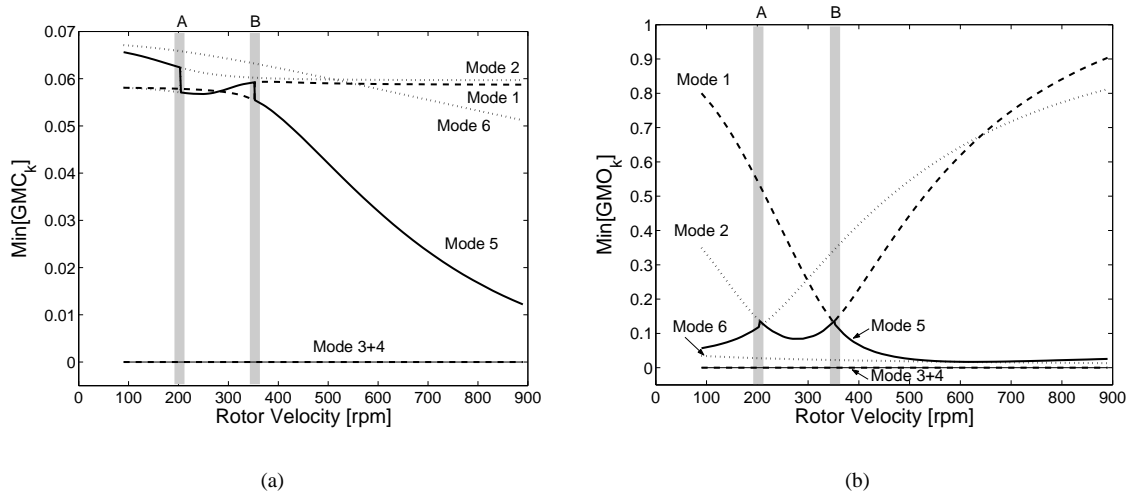


Figure 4: Indices of modal controllability (a) and observability (b) for the tuned rotor-blade system.

## 5.2. Mistuned system analysis

In the introduction it was described that bladed disk coupled vibrations can be controlled and monitored by using only shaft-based actuation and sensing, if the blades are properly mistuned. Blades can be mistuned by varying their modulus of elasticity, their length, their weight etc.. Throughout this study the bladed disk is mistuned by varying the size of the blade tip masses. Onto the tip mass of blade number two is added 10% extra mass, to the third blade 20% and to the fourth blade 30%. The rotor unbalance such mistuning will introduce is compensated by adding extra balancing mass directly onto the disk.

Similar to the case of the tuned bladed disk, first, the dynamical properties and the influence of the mistuning are observed by numerical simulation. Figures 5 and 6 show waterfall diagrams and the relation of each frequency component to its respective mode. The most significant changes of the dynamical response caused by the introduction of deliberate mistuning, compared to the tuned system responses in Fig. 2, can be detected in the response of the rotor lateral motion. Figure 6 clearly shows that the blade mistuning results in an increased number of parametric mode components in the rotor movement, R3 to R6 and P3 to P6. Four forward rotating and four backward rotating mode components related to the motion of the blades are observed in the rotor motion. All four primarily blade related mode shapes become coupled to rotor lateral motion. This indicates that all primarily blade related modes might become detectable and controllable by monitoring and acting onto the rotor in the inertial frame by using an active bearing. A total of eight mode shape transition regions can be detected for the completely mistuned bladed disk resulting in an equal number of mode shape interaction regions at the speeds 81 rpm (A), 102 rpm (B), 138 rpm (C), 168 rpm (D), 235 rpm (E), 258 rpm (F), 305 rpm (G) and 355 rpm (H).

Figure 7 shows quantitative measures of modal controllability and observability as functions of the rotational speed for the deliberately mistuned system. The indices are only shown for angular velocities higher than 160 rpm due to some difficulties related to the separation of basis and redundant solutions obtained when solving the time-variant eigenvalue problem for the system rotating at a low angular velocity. While the speed decreases the imaginary parts of the eigenvalues decrease as well. Moreover, the mistuning will distinguish the basis eigenvalues imaginary parts slightly. These factors

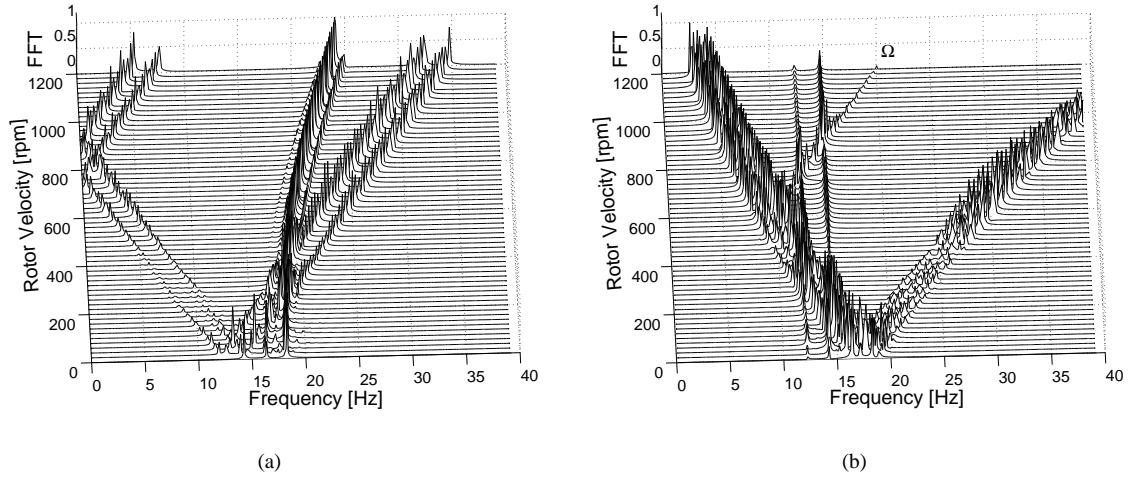


Figure 5: Waterfall diagrams of the blade (a) and the rotor movement (b) for the mistuned rotor-blade system.

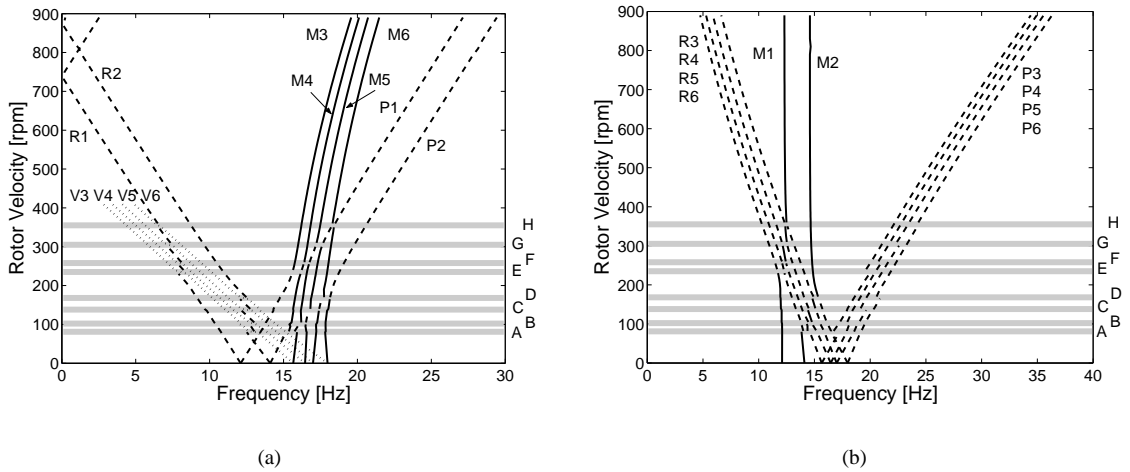


Figure 6: Basis (—) and parametric eigenvalues of order  $\pm 1$  (— —) and of order  $-2$  ( $\cdot \cdot \cdot$ ) for the blade (a) respectively rotor movement (b) when the blades are deliberately mistuned.

imply that the basis eigenvalues of the system will tend to coincide with redundant eigenvalues making the separation process of the basis eigenvalues and vectors a very difficult task. Consequently, the controllability and observability indices of Fig. 7 are cut off at 160 rpm.

The limitation of the angular velocity at 160 rpm hinders a complete analysis of the controllability and observability during the entire mode shape crossing region. However, the trends of the indices and the interaction among the basis and parametric mode shape components can be observed. As it was detected by the modal analysis, it is seen that all six modes are controllable by only shaft actuation, as a consequence of the deliberate blade mistuning even though the indices indicate only a minor degree of controllability. It is noticed that, for increasing velocities, the controllability indices of the modes 3 to 6 are decreasing while the level of controllability of the modes 1 and 2 are almost constant. This is due to the fact that the vibration coupling among disc and blades reduces. The controllability indices of the modes 1 and 2 tend to converge towards the same steady levels as for the tuned system of Fig. 4. The observability indices show that the system are also, to some extent and at some velocities, observable from disc movement measurements. The observability indices of the first two modes are very similar to the values obtained for the tuned system shown in Fig. 4. Due to the decreasing vibration coupling, it is seen that the modes 3 to 6 become non-observable for increasing speeds. This implies that the rotational speed becomes of crucial importance while analysing the controllability and observability using only shaft actuation and sensing.

The levels of controllability and observability depend on the degree of mistuning. Figure 8 shows the controllability and observability indices of the least controllable and observable mode as functions of the percentage level of the blade tip mass mistuning. The mass of the  $i$ 'th tip mass is given by  $m_{ti} = (1 + (i - 1)\mu)m_{t1}$  for  $i = 1, 2, 3, 4$  where  $\mu$  is the percentage of mistuning and  $m_{t1}$  is the tip mass of blade 1. At first one would think, that increasing the level of blade mistuning would enhance the levels of controllability and observability. However, observing the indices it seems like the controllability tend to converge towards steady levels as the level of mistuning are increased towards "infinity".

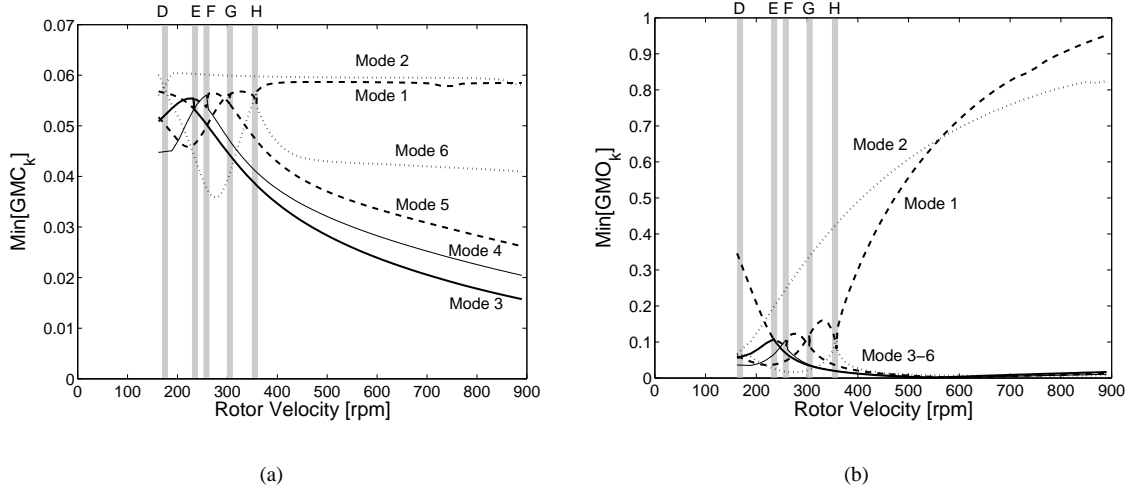


Figure 7: Indices of modal controllability (a) and observability (b) for the mistuned rotor-blade system.

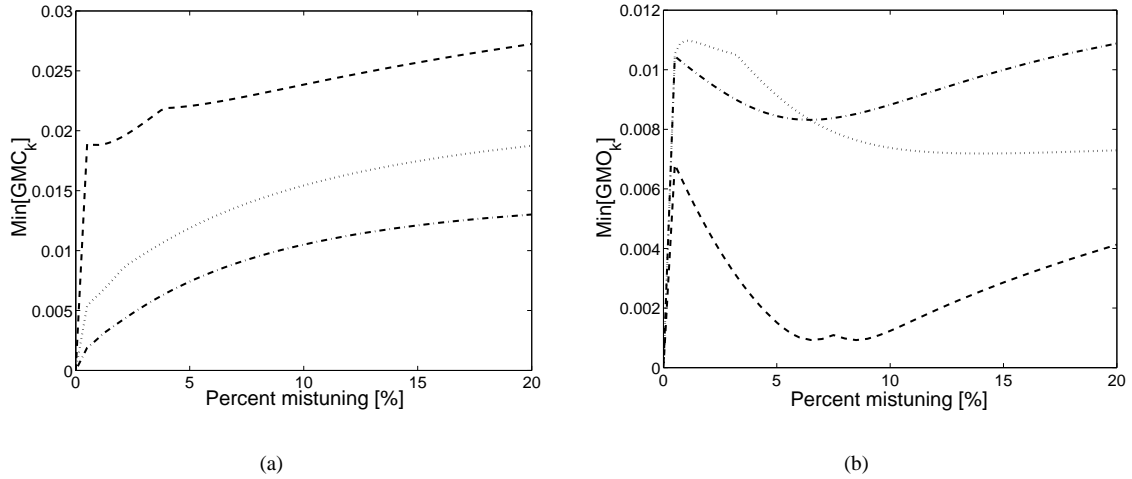


Figure 8: Minimum index of modal controllability (a) and observability (b) as function of the degree of blade tip mass mistuning.  $\Omega = 600$  rpm (---);  $\Omega = 900$  rpm ( $\cdots$ ) and  $\Omega = 1200$  rpm (- · -).

Increasing the degree of mistuning by means of adding more mass to the blades implies that the vibration coupling among disk and blades should be increased. On the other hand increasing the masses enhance the centrifugal stiffening of the blades having an opposing effect on the vibration coupling. Regarding the observability indices no definitive conclusion can be deducted, however, it is noticed that the very small and depend strongly on the angular speed. The conclusion is, that an upper limits exist of how controllable and observable a system can be done by introducing mistuning.

## 6. Experimental control results

To study the feasibility of rotor-blade coupled vibration control via shaft-based actuation, an active control scheme is applied to the experimental test facility. As it was described in the introduction, the active controller can be designed and implemented using one of two very different strategies, i.e. an absorbing strategy or a forcing strategy. The first one of these two strategies, the absorbing strategy, is based on suppressing blade vibrations by means of suppressing the vibrations of the rotor. The blade vibration energy can be absorbed via shaft vibration control due to the vibration coupling between rotor and blades, however, the use of such a strategy requires significant vibration coupling. The alternative forcing strategy is based on the principle of forcing the movement of the rotor in order to minimize the deflections of the blades. Such strategy will be applicable to systems with a low degree of vibration coupling but it will also inevitable mean that a time-variant control algorithm, encountering the time-variant distribution of inertia, has to be implemented. Such a strategy was adopted in (Christensen and Santos, 2004a,b) where a periodic modal state feedback controller was designed and implemented. However, several typical problems related to practical implementation of state feedback controllers relying heavily on quantitative model information were identified, i.e. lack of robustness and a high sensitivity to model uncertainties. Consequently, for the system under consideration in this study presenting significant coupling between rotor and blade motions, a simple control strategy is adopted composed of two independent shaft-based PD-controllers. Figure 9 shows schematically the control system setup. Rotor lateral movements are measured in two orthogonal directions and the sensed displacements are fed back into the two PD-controllers. The control signals are sent through power amplifiers

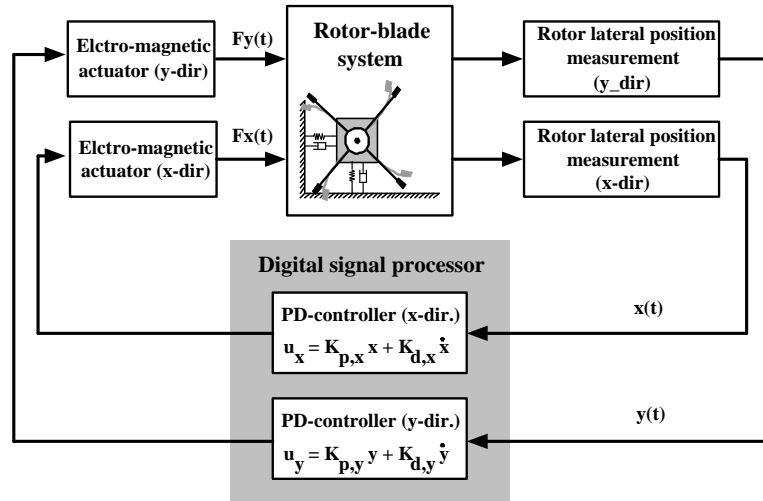


Figure 9: Schematic drawing of the PD-controlled rotor-blade system.

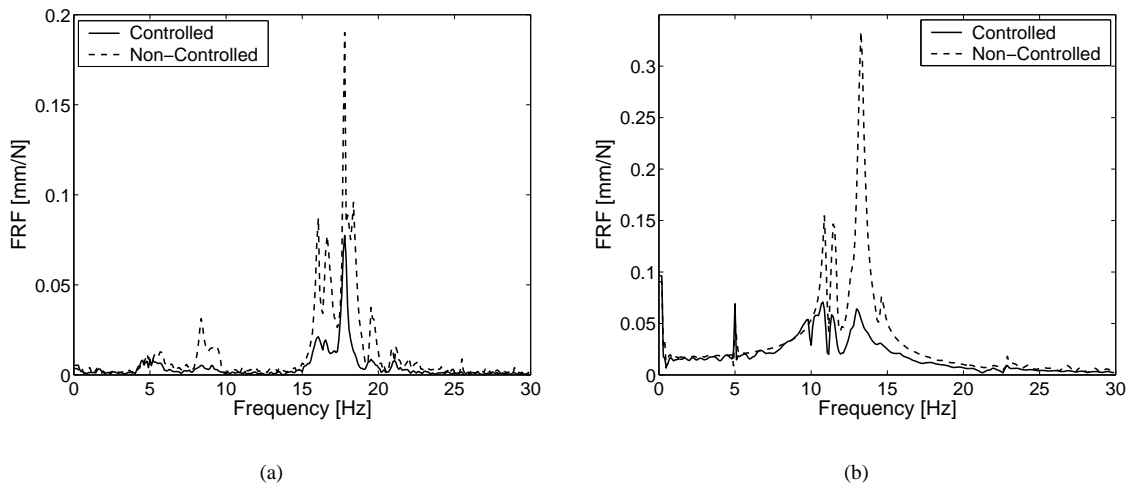


Figure 10: Experimental frequency response functions of blade (a) and rotor lateral motion (b) for the non-controlled (---) and actively controlled (—) rotor-blade system ( $\Omega = 300$  rpm).

to the electro-magnetic actuators. Figure 10 shows experimentally measured frequency response functions of the rotor and blade motion for the active controlled rotor-blade system rotating at the constant velocity  $\Omega = 300$  rpm compared to the passively running system. These responses reveal a significant reduction of the rotor as well as the blade vibration levels.

## 7. Conclusion

In this paper, shaft-based active control of rotor-blade coupled vibrations has been studied. The modal controllability and observability were studied and the necessity of introducing deliberate blade mistuning in order to make all vibration modes controllable and observable, via the shaft-based actuation and sensing, was shown. Moreover, the results reveal that the dynamical characteristics and the levels of controllability and observability change significantly as function of the angular velocity. More specifically, when the bladed rotor rotates at certain velocities where parametric and basis vibration modes interact with themselves. The rotor-blade vibration coupling, resulting in such parametric vibrations, has to be taken into consideration when implementing active controls. Furthermore, limits exist of how controllable and observable a bladed rotor can become via the introduction of deliberate blade mistuning. Finally, experimental results reveal the potential of controlling blade vibrations by using active controlled bearings, though, such control requires significant vibration coupling among rotor and blades in order to be efficient.

## 8. References

- Al-Bedoor, B.O., 2002, "Blade Vibration Measurement in Turbo-Machinery: Current Status", The Shock and Vibration Digest, Vol. 34, No. 6, pp. 455-461.
- Alizadeh, A., Ehmann C., Schönhoff, U., Nordmann, R., 2003, "Active Bearing of Rotors Utilizing Robust Controlled Piezo Actuators", Proceedings of ASME DETC'03, paper DETC2003/VIB-48850, Chicago, Illinois, USA.
- Althaus, J., Ulbrich, H., 1992, "A Fast Hydraulic Actuator for Active Vibration Control", Proceedings of The Fifth

International Conference on Vibrations in Rotating Machinery, Bath, England.

- Christensen, R.H., Santos, I.F., 2004a, "A Study of Active Rotor-Blade Vibration Control Using Electro-Magnetic Actuation - Part 1: Theory", Proceedings of ASME/IGTI Turbo Expo 2004, paper GT2004-53509, Vienna, Austria.
- Christensen, R.H., Santos, I.F., 2004b, "A Study of Active Rotor-Blade Vibration Control Using Electro-Magnetic Actuation - Part 2: Experiments", Proceedings of ASME/IGTI Turbo Expo 2004, paper GT2004-53512, Vienna, Austria.
- Christensen, R.H., Santos, I.F., (in press), "Design of Active Controlled Rotor-Blade Systems Based on Time-Variant Modal Analysis", *Journal of Sound and Vibration*.
- Christensen, R.H., Santos, I.F., 2004c, "Methodology for Analysing Controllability and Observability of Bladed Disc Coupled Vibrations", Proceedings of the Eleventh International Congress on Sound and Vibration, St. Petersburg, Russia.
- Hamdan, A.M.A., Nayfeh, A.H., 1989, "Measure of Modal Controllability and Observability for First- and Second-Order Linear Systems", *Journal of Guidance, Control and Dynamics*, Vol. 12, No. 3, pp. 421-428.
- Kenyon, J.A., Griffin, J.H., Kim, N.E., 2004, "Sensitivity of Tuned Bladed Disk Response to Frequency Veering", Proceedings of ASME/IGTI Turbo Expo 2004, paper GT2004-53280, Vienna, Austria.
- Santos, I.F., Saracho, C.M., Smith, J.T., Eiland, J., 2004, "Contribution to Experimental Validation of Linear and Non-linear Dynamic Models for Representing Rotor-Blade Parametric Vibrations", *Journal of Sound and Vibration*, Vol 271, No. 3-5, pp. 883-904.
- Santos, I.F., Scalabrin, A., 2003, "Control System Design for Active Lubrication with Theoretical and Experimental Examples", *ASME Journal of Engineering for Gas Turbines and Power*, Vol. 125, No. 1, pp. 75-80.
- Saracho, C.M., Santos, I.F., 2003, "Modal analysis in periodic, time-varying systems with emphasis to the coupling between flexible rotating beams and non-rotating flexible structures", Proceedings of the X International Symposium on Dynamic Problems of Mechanics, pp. 399-404, São Paulo, Brazil.
- Schweitzer, G., 1998, "Magnetic Bearings as a Component of Smart Rotating Machinery", Proceedings of The Fifth International Conference on Rotor Dynamics, pp. 3-15, Darmstadt, Germany.
- Szász, G., Flowers, G.T., Hartfield, R.J., 2000, "Hub-Based Vibration Control of Multiple Rotating Airfoils", *Journal of Propulsion and Power*, Vol. 16, No. 6, pp. 1155-1163.
- Szász, G., Flowers, G.T., 2001, "Time Periodic Control of a Bladed Disk Assembly Using Shaft Based Actuation", *Journal of Vibration and Acoustics*, Vol. 123, pp. 395-401.
- Szász, G., Flowers, G.T., 2000, "Vibration Suppression in Bladed-Disk Assemblies With Deliberate Mistuning via Magnetic Bearings", *Journal of Vibration and Control*, Vol. 6, pp. 903-921.
- Xu, J., Gasch, R., 1995, "Modale Behandlung linearer periodisch zeitvarianter Bewegungsgleichungen", *Archive of Applied Mechanics*, Vol. 65, No. 3, pp. 178-193, (in German).
- Zielinski, M., Ziller, G., 2000, "Noncontact Vibration Measurements on Compressor Rotor Blades", *Measurement Science Technology*, Vol. 11, pp. 847-856.

## 9. Responsibility Notice

The authors are the only responsible for the printed material included in this paper.